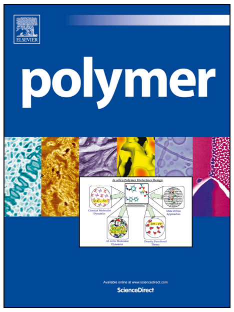

Aliphatic polyketones via cross-metathesis polymerization: Synthesis and post-polymerization modification

Fu-Rong Zeng, Jing Xu, Qi Xiong, Kai-Xuan Qin, Wei-Jun Xu, Yue-Xin Wang, Zan-Jiao Liu, Zi-Long Li, Zi-Chen Li

PII: S0032-3861(19)30942-5

DOI: https://doi.org/10.1016/j.polymer.2019.121936

Reference: JPOL 121936

To appear in: *Polymer*

Received Date: 22 August 2019

Revised Date: 20 October 2019

Accepted Date: 21 October 2019

Please cite this article as: Zeng F-R, Xu J, Xiong Q, Qin K-X, Xu W-J, Wang Y-X, Liu Z-J, Li Z-L, Li Z-C, Aliphatic polyketones via cross-metathesis polymerization: Synthesis and post-polymerization modification, *Polymer* (2019), doi: https://doi.org/10.1016/j.polymer.2019.121936.

Graphical Abstract

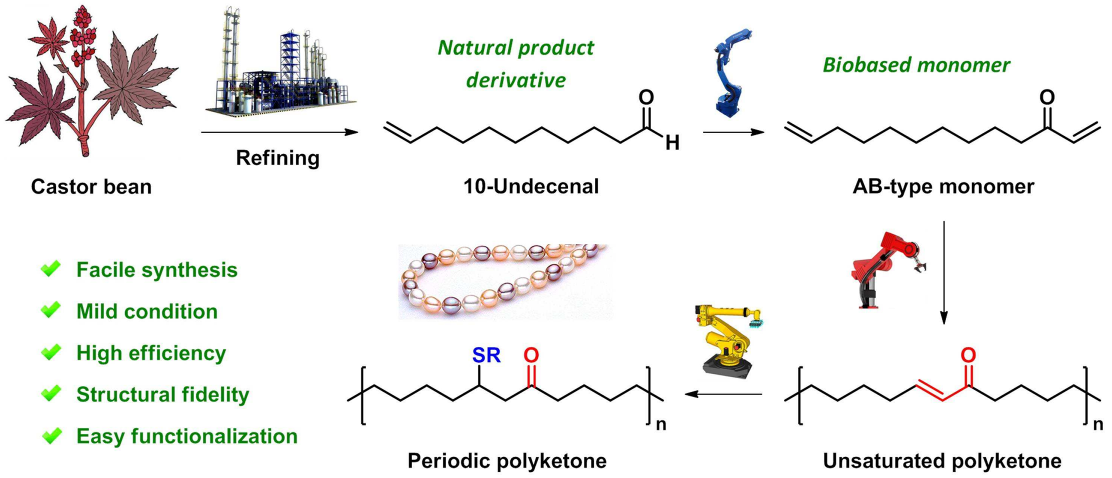

Manuscript submitted to *Polymer* as an article

Aliphatic Polyketones via Cross-Metathesis Polymerization: Synthesis and Post-Polymerization Modification

Fu-Rong Zeng[a], Jing Xu[b], Qi Xiong[a], Kai-Xuan Qin[a], Wei-Jun Xu[a], Yue-Xin Wang[a], Zan-Jiao Liu[a], Zi-Long Li[a,]*, Zi-Chen Li[c]

[a] *Department of Chemistry, College of Science, Huazhong Agricultural University, Wuhan 430070, Hubei, China*

[b] *College of Materials Science and Engineering, Key Laboratory of Textile Fiber and Products (Ministry of Education), Wuhan Textile University, Wuhan 430200, Hubei, China*

[c] *Beijing National Laboratory for Molecular Sciences (BNLMS), Key Laboratory of Polymer Chemistry & Physics of Ministry of Education, Department of Polymer Science & Engineering, College of Chemistry and Molecular Engineering, Peking University, Beijing 100871, China*

* Corresponding author:

E-mail address: lizilong@mail.hzau.edu.cn (Z.-L. Li)

Abstract

Polyolefins attract considerable attention due to their vast consumption and wide application. In this study, cross-metathesis polymerization (CMP) is demonstrated to be an efficient and feasible method for the synthesis of aliphatic polyketones. The synthetic route features good yield, mild condition and easy operation. The success of CMP relies on the high cross-metathesis tendency between α-olefin and vinyl ketone units of monomer **2**. Optimization of polymerization condition was conducted to generate unsaturated polyketone **P0** ($M_{n,GPC}$ = 14 kDa), and the results of kinetic study verified high efficiency and structural integrity of this system. Furthermore, post-polymerization modification of **P0** by using thiol-Michael chemistry furnished functional polyketones **P1**-**P6**, and full conversion of the internal vinyl ketone groups of **P0** was observed in each case. The pristine and functional polyketones **P0**-**P6** were virtually soluble in most common organic solvents. In particular, hydrophobic and fluorescent polyketones (**P5** and **P6**) were also obtained by this means. Therefore, this synthetic strategy shows promising future and exemplifies huge potential for the synthesis of a diverse range of functional polyketones.

Keywords

Aliphatic polyketones

Cross-metathesis polymerization

Thiol-Michael chemistry

1. Introduction

Copolymers of ethylene and polar monomers attract considerable attention due to their broad range of applications [1-3]. Even low incorporation of polar groups will significantly influence the performance of polyolefins [4]. In particular, aliphatic polyketones have become a research focus recently due to their unique properties such as crystallinity, thermal stability, high stiffness, corrosion resistance and photo degradability [5]. Meanwhile, a number of preparative approaches have been developed over the last decades. For example, free radical copolymerization of ethylene and CO generally leads to low content of CO and a high degree of branching [6]. Linear polyketones can be synthesized by using insertion copolymerization in the presence of palladium catalysts [7-14]. It is noteworthy that this method is by far the most reliable one for the synthesis alternating polyketones [15-17]. However, this technique still faces challenges such as generation of homopolyolefins and methyl branches [18]. Therefore, control over microstructure is still an urgent demand for the synthesis of aliphatic polyketones.

The above issue has been partially addressed with the advent of metathesis polymerization [19,20]. For example, defect-free model polyketones were obtained through acyclic diene metathesis (ADMET) polymerization although vacuum, high temperature and rather long reaction time were basically required [21,22]. Later on, precision polyketone with regular spacing was generated by ring-opening metathesis polymerization (ROMP) [23,24]. In this case, low conversion was observed as a result of chain transfer. It is notable that ADMET and ROMP systems suffer from insolubility of saturated polyketones in most common organic solvents. Moreover, main chain functionalization of aliphatic polyketone is scarcely reported probably due to the lack of reactive sites [25].

In this work, we propose cross-metathesis polymerization (CMP) as an efficient and feasible technique for the synthesis of linear polyketones with definite structures. Biobased monomer **2** bearing α-olefin and vinyl ketone terminuses were synthesized in two steps. Following CMP of monomer **2**, the resulting unsaturated polyketone **P0** underwent post-polymerization modification to furnish functional polyketones **P1**-**P6**. Thiol-Michael addition under proper condition enabled full conversion of the internal alkene units of **P0** in each case. Ultimately, soluble polyketones with diverse pendent groups such as fluorophore and perfluorocarbon were readily obtained.

2. Experimental

2.1. Materials

10-Undecenal (97%, Adamas-beta), vinylmagnesium bromide (1 mol L^{-1} in dry tetrahydrofuran, Aladdin), 2-iodoxybenzoic acid (IBX, 95%+, Adamas-beta), 3-octen-2-one (>96%, TCI), 1-butanethiol (97%, Aladdin), benzyl mercaptan (98%, Aladdin), methyl thioglycolate (>98%, TCI), 4-methylthiophenol (98%, Aladdin), 1H,1H,2H,2H-perfluorodecanethiol (97%, Aladdin), 8-mercaptoquinoline hydrochloride (95%, TCI), dimethylphenylphosphine (DMPP, 97%, Alfa Aesar), Hoveyda-Grubbs second generation catalyst (HG-II, 97%, Sigma-Aldrich), 1,4-benzoquinone (BQ, 99%, Innochem), ethyl vinyl ether (EVE, 98%, stabilized with

0.1% KOH, Aladdin), tetrahydrofuran (THF, 99.0%, Sinopharm), dimethyl sulfoxide (DMSO, ≥99%, Sinopharm), *N*,*N*-dimethylformamide (DMF, ≥99.5%, Sinopharm), toluene (TOL, 99.5%, Sinopharm), dichloromethane (DCM, 99.5%, Sinopharm), chloroform (TCM, 99.5%, Sinopharm), petroleum ether (petrol, 60-90 ^{o}C, 99.7%, Sinopharm), ethyl acetate (EtOAc, ≥99.6%, Sinopharm), diethyl ether (≥99.7%, Sinopharm), methanol (≥99.5%, Sinopharm), magnesium sulfate anhydrous ($MgSO_4$, ≥98.0%, Chinasun), sodium chloride (≥99.5%, Sinopharm), silica gel (reagent grade, 200-300 mesh, Qingdao Haiyang Chemical Co., Ltd), calcium chloride anhydrous ($CaCl_2$, ≥98.0%, Sinopharm), calcium hydride (CaH_2, ≥97.0%, Tianjin Chemical Reagent Research Institute Co., Ltd) and deuterated chloroform ($CDCl_3$, 99.8% deuteration, 0.03 % v/v tetramethylsilane (TMS) and silver foil, Cambridge Isotope Laboratories, Inc) were used as received unless otherwise noted. Argon gas (99.9%) was obtained from Wuhan Minghui Gas Technology Co., Ltd. THF was refluxed with sodium for 8 h and distilled. DMF was vigorously stirred with CaH_2 for 6 h and distilled *in vacuo*. TOL, DCM and TCM were all degassed by sonication for 5 min prior to polymerization.

2.2. Characterization

Bruker Avance 600 spectrometer was used to measure the ^{1}H (600 MHz) and ^{13}C (150 MHz) NMR spectra. All the samples were dissolved in $CDCl_3$ with TMS as the internal reference for chemical shifts. Number-average molecular weights ($M_{n,GPC}$) and polydispersity indices ($Đ$) were measured by gel permeation chromatography (GPC). The measurements were conducted in THF (flow rate: 1 ml min^{-1}) at 35 ^{o}C with

Waters 1525 binary HPLC pump equipped with a Waters 2414 refractive index detector and three Waters Styragel columns (1×10^4, 1×10^3, and 500 Å pore sizes). A series of narrowly dispersed polystyrenes were used as the standards, and Breeze 3.30 SPA software was used to calculate the $M_{\mathrm{n,GPC}}$ and $Đ$ values. Electrospray ionization mass spectroscopy (ESI-MS) characterization was conducted by using a Bruker APEX-IV Fourier transform mass spectrometer in positive ion mode. Thermal gravimetric analysis (TGA) was carried out by using a Q600-SDT thermo-gravimetric analyzer (TA Co., Ltd.) with nitrogen purging rate of 100 ml min^{-1}. Measurement was conducted from ambient temperature to 600 $^{\mathrm{o}}$C at a heating rate of 10 $^{\mathrm{o}}$C min^{-1}. Differential scanning calorimetry (DSC) characterizations were carried out by using a Q100 differential scanning calorimeter (TA Co., Ltd.) with nitrogen purging rate of 50 ml min^{-1}. The program was set to finish two cycles within temperature range from -80 $^{\mathrm{o}}$C to 80/120 $^{\mathrm{o}}$C. The heating or cooling rate was 10 $^{\mathrm{o}}$C min^{-1}. Data of the endothermic curve was acquired from the second scan. TA Universal Analysis software was used for data acquisition and processing in TGA and DSC measurements. Wide angle powder X-ray diffraction (WAXD) data were obtained by using a Bruker D8 ADVANCE diffractomer at 40 kV and 50 mA (copper K_α radiation with $\lambda = 1.54$ Å). All the measurements were conducted at room temperature with a scanning rate of 10^{o} min^{-1} over 2θ ranges from 5^{o} to 85^{o}. Polymer solutions of **P0** and **P5** (10 mg mL^{-1} in TCM) were spin coated at 1500 rpm for 20 s onto glass wafers. The static contact angle of a 2 μL water droplet deposited on a spin-coated surface was measured. The results are the average of ten measurements. UV-Vis spectra were recorded by using a UV-Vis spectrophotometer UV-2601 (Shimadzu) at ambient temperature within wavelength (λ) range from 280 nm to 400 nm. Fluorescence spectra were recorded by using a Hitachi F-7000 fluorescence spectrometer at room temperature within wavelength (λ) range from 360 nm to 600 nm. The scanning rate was 240 nm min^{-1}, and the excitation and emission slit widths were both 5.0 nm.

2.3. Synthesis of monomer precursor ***1***

10-Undecenal (5.05 g, 30 mmol) and dry THF (40 mL) were added to a 250 mL round bottom flask and cooled to -20 ^{o}C under Ar. Vinylmagnesium bromide (45 mL, 1 mol L^{-1} in dry THF) was added, and the mixture was stirred at 0 ^{o}C for 1 h. At this time, the light yellow solution was warmed to ambient temperature. Afterward, saturated ammonium chloride solution (50 mL) was added, and the mixture was vigorously stirred for 5 min. The mixture was extracted by EtOAc (twice), and the combined organic phase was washed with brine, dried over $MgSO_4$ followed by filtration and removal of solvent to furnish viscous colorless oil. The crude product was purified by silica gel column chromatography (petrol/EtOAc = 30/1) to generate monomer precursor **1** as a viscous colorless oil (3.83 g, 19.5 mmol). Production yield: 65%. ^{1}H NMR (600 MHz, $CDCl_3$), δ (TMS, ppm): 5.78-5.90 (m, 2H), 5.20-5.24 (dt, *J* = 17.2, 1.3 Hz, 1H), 5.09-5.11 (m, 1H), 4.97-5.01 (ddd, *J* = 17.1, 3.4, 1.6 Hz, 1H), 4.92-4.94 (m, 1H), 4.06-4.13 (dd, *J* = 14.5, 9.9 Hz, 1H), 2.02-2.06 (m, 2H), 1.50-1.57 (tdt, *J* = 11.4, 7.8, 3.9 Hz, 2H), 1.47-1.59 (d, *J* = 4.1 Hz, 1H), 1.34-1.42 (m, 2H), 1.25-1.34 (m, 10H). ^{13}C NMR (150 MHz, $CDCl_3$): δ 141.35, 139.23, 114.53, 114.12, 73.29, 37.05, 33.81, 29.54, 29.52, 29.42, 29.12, 28.92, 25.33. ESI-MS: [M + H$^+$] = $C_{13}H_{25}O$, calcd: 197.190545, found: 197.190600.

*2.4. Synthesis of monomer **2***

IBX (6.72 g, 24 mmol) and DMSO (30 mL) were added to a 150 mL round bottom flask to generate solution 1. Precursor **1** (3.92 g, 20 mmol) was dissolved in THF (30 mL) to obtain solution 2, which was dropwise added to solution 1. The mixture was stirred at room temperature for 2 h. At this time, water (20 mL) was added under stirring, and white solid was observed. After filtration, the mixture was extracted by EtOAc (twice), and the combined organic phase was washed with brine, dried over $MgSO_4$ followed by filtration and removal of solvent to furnish viscous colorless oil. The crude product was purified by silica gel column chromatography (petrol/EtOAc = 50/1) to give monomer **2** as a viscous colorless oil (2.85 g, 14.7 mmol). Production yield: 74%. ^{1}H NMR (600 MHz, $CDCl_3$), δ (TMS, ppm): 6.33-6.38 (dd, J = 17.7, 10.6 Hz, 1H), 6.20-6.23 (d, J = 17.6 Hz, 1H), 5.77-5.84 (m, 2H), 4.97-5.01 (dd, J = 17.1, 1.1 Hz, 1H), 4.92-4.94 (d, J = 10.1 Hz, 1H), 2.56-2.59 (t, J = 7.4 Hz, 2H), 2.02-2.05 (q, J = 7.1 Hz, 2H), 1.59-1.64 (m, 2H), 1.34-1.39 (dd, J = 13.5, 6.7 Hz, 2H), 1.23-1.34 (s, 8H). ^{13}C NMR (150 MHz, $CDCl_3$): δ 201.13, 139.20, 136.62, 127.86, 114.15, 39.66, 33.79, 29.37, 29.31, 29.25, 29.07, 28.90, 24.01. ESI-MS: [M + H$^+$] = $C_{13}H_{23}O$, calcd: 195.174342, found: 195.174227.

2.5. Model reactions

Take the synthesis of 4-(benzylthio)octan-2-one as an example.

3-octen-2-one (126 mg, 1 mmol) was dissolved in DMF (5 mL) in a 10 mL round bottom flask. At this time, benzyl mercaptan (234 μL, 2 mmol) and DMPP (1.5 μL, 10 μmol) were added, and the mixture was stirred at room temperature for 24 h, at which time TLC showed that 3-octen-2-one was fully converted. EtOAc was added to the system, and the organic phase was washed by water and brine, dried over $MgSO_4$ followed by filtration and removal of solvent to give viscous colorless oil. The crude product was purified by silica gel column chromatography (petrol/EtOAc = 30/1) to give the desired product as a viscous colorless oil in nearly quantitative yield. ^{1}H NMR (600 MHz, $CDCl_3$), δ (TMS, ppm): 7.29-7.33 (m, 4H), 7.22-7.24 (t, J = 6.9 Hz, 1H), 3.71-3.76 (m, 2H), 3.01-3.06 (p, J = 6.8 Hz, 1H), 2.57-2.68 (ddd, J = 39.2, 16.8, 6.9 Hz, 2H), 2.08 (s, 3H), 1.47-1.53 (m, 2H), 1.21-1.39 (m, 4H), 0.85-0.87 (t, J = 7.2 Hz, 3H). ^{13}C NMR (150 MHz, $CDCl_3$): δ 206.98, 138.53, 128.92, 128.48, 126.99, 49.65, 40.43, 35.77, 34.84, 30.54, 28.81, 22.45, 13.98. ESI-MS: $[M + H^+] = C_{15}H_{23}OS$, calcd: 251.146413, found: 251.145803; $[M + NH_4^+] = C_{15}H_{26}ONS$, calcd: 268.172962, found: 268.172258.

Likewise, the synthesis of thiol-Michael adducts 4-(butylthio)octan-2-one, methyl 2-((2-oxooctan-4-yl)thio)acetate and 4-(*p*-tolylthio)octan-2-one was carried out similarly. Notably, the amount of methyl thioglycolate was 120 mol% with respect to substrate 3-octen-2-one. Meanwhile, 4-(*p*-tolylthio)octan-2-one was obtained in about 40% yield, and only partial consumption of 3-octen-2-one was observed as reflected by TLC. Fortunately, full conversion of 3-octen-2-one could be achieved if a large excess of 4-methylthiophenol (600 mol% with respect to 3-octen-2-one) was used. These compounds were all viscous colorless oils.

NMR and ESI-MS data of 4-(butylthio)octan-2-one:

^{1}H NMR (600 MHz, $CDCl_3$), δ (TMS, ppm): 3.06-3.11 (m, 1H), 2.62-2.73 (m, 2H), 2.47-2.54 (m, 2H), 2.18 (s, 3H), 1.51-1.57 (m, 4H), 1.22-1.47 (m, 6H), 0.89-0.92 (m, 6H). ^{13}C NMR (150 MHz, $CDCl_3$): δ 207.17, 49.74, 40.60, 35.08, 31.84, 30.82, 30.63, 28.98, 22.55, 22.08, 14.00, 13.68. ESI-MS: [M + H$^+$] = $C_{12}H_{25}OS$, calcd: 217.162063, found: 217.161955.

NMR and ESI-MS data of methyl 2-((2-oxooctan-4-yl)thio)acetate:

^{1}H NMR (600 MHz, $CDCl_3$), δ (TMS, ppm): 3.74 (s, 3H), 3.22-3.32 (m, 3H), 2.65-2.81 (ddd, J = 23.5, 17.2, 6.8 Hz, 2H), 2.17 (s, 3H), 1.51-1.61 (m, 2H), 1.25-1.47 (m, 4H), 0.89-0.91 (t, J = 7.2 Hz, 3H). ^{13}C NMR (150 MHz, $CDCl_3$): δ 206.55, 171.14, 52.40, 49.41, 41.38, 34.60, 32.86, 30.54, 28.83, 22.44, 13.95. ESI-MS: [M + H$^+$] = $C_{11}H_{21}O_3S$, calcd: 233.120592, found: 233.120575; [M + NH_4^+] = $C_{11}H_{24}O_3NS$, calcd: 250.147141, found: 250.147081; [M + Na$^+$] = $C_{11}H_{20}O_3SNa$, calcd: 255.102536, found: 255.102615; [M + K$^+$] = $C_{11}H_{20}O_3SK$, calcd: 271.076474, found: 271.076551.

NMR and ESI-MS data of 4-(p-tolylthio)octan-2-one:

^{1}H NMR (600 MHz, $CDCl_3$), δ (TMS, ppm): 7.30-7.32 (d, J = 8.1 Hz, 2H), 7.10-7.11 (d, J = 7.9 Hz, 2H), 3.47-3.51 (m, 1H), 2.58-2.71 (ddd, J = 24.4, 17.0, 6.8 Hz, 2H), 2.33 (s, 3H), 2.12 (s, 3H), 1.38-1.58 (m, 4H), 1.23-1.36 (m, 2H), 0.87-0.90 (t, J = 7.3 Hz, 3H). ^{13}C NMR (150 MHz, $CDCl_3$): δ 207.00, 137.46, 133.20, 130.45, 129.71, 49.11, 44.11, 34.39, 30.64, 29.03, 22.47, 21.11, 13.98. ESI-MS: [M + H$^+$] = $C_{15}H_{23}OS$, calcd:

251.146413, found: 251.145914; [M + NH_4^+] = $C_{15}H_{26}ONS$, calcd: 268.172962, found: 268.172419.

2.6. Optimization of CMP condition

Take the procedure of run 1 as an example.

Monomer **2** (97 mg, 0.5 mmol) and BQ (0.5 mg, 5 μmol) were weighed in a 25 mL Schlenk flask equipped with a Teflon valve. TOL (0.5 mL) was added to form solution 1, which was placed in 80 °C oil bath. HG-II catalyst (1.6 mg, 2.5 μmol) was dissolved in TOL (0.5 mL) to furnish green solution 2. At this time, solution 2 was rapidly mixed with solution 1 under argon ([**2**] = 0.5 mol L^{-1}). The flask was connected to a reflux condenser which was equipped with an anhydrous $CaCl_2$ loaded drying tube. The polymerization solution was stirred at 80 °C for 12 h. Argon was supplied through the Teflon valve. No precipitation of polyketone or apparent evaporation of TOL was observed throughout the polymerization process. EVE (0.5 mL) was added under argon to terminate the polymerization, and the solution was stirred for an additional 5 min. The polymer solution was poured into ice-cold methanol (100 mL) to generate brownish precipitate. After centrifugation and vacuum dryness, polymer was obtained as a brownish solid in 88% yield.

Samples for run 2-7 were synthesized similarly.

2.7. Polymerization kinetics

The synthetic procedure was similar to that of optimization of CMP condition (run 7). Specifically, an aliquot solution of **P0** was taken at 0.5 h, 1 h, 2 h, 3 h, 4 h, 6 h, 8 h, 12 h and 24 h followed by termination and removal of volatiles prior to ^{1}H NMR characterization.

2.8. Post-polymerization modification

Take the synthesis of polymer **P2** as an example.

Polymer **P0** (194 mg, 1 mmol vinyl ketone), TCM (5 mL) and DMF (5 mL) were mixed in a 25 mL round bottom flask to form a brownish solution. Afterward, benzyl mercaptan (725 μL, 6 mmol) and DMPP (1.5 μL, 10 μmol) were added. The mixture was stirred at 50 ^{o}C for 48 h. At this time, the solution was poured into cold methanol (100 mL) and stored at 4 ^{o}C overnight to give brownish semi-solid. Precipitation was conducted for three times to completely remove excessive thiol and DMF. After centrifugation and vacuum dryness, polymer **P2** was obtained as a viscous semi-solid in about 90% yield.

Polymers **P1** and **P3**-**P6** were synthesized similarly. These samples were viscous semi-solids.

3. Results and discussions

3.1. Monomer synthesis

A two-step synthetic route of monomer **2** was depicted in Scheme 1, and a natural product derivative 10-undecenal was selected as the starting material. This compound is derived by pyrolysis and reduction from castor oil [26,27], which has been used for the synthesis of poly-α,β-unsaturated aldehydes [28] and bifunctional aldehyde derivatives [29]. According to olefin categorization proposed by Grubbs [30], terminal alkene and vinyl ketone are type I and II olefins, respectively. Consequently, compound **2** is an AB-type monomer featuring head-to-tail polycondensation. At first, intermediate **1** was obtained through Grignard reaction between 10-undecenal and vinylmagnesium bromide in dry THF. Subsequently, monomer **2** was synthesized via oxidation of precursor **1** in mixed solvent by using IBX as the oxidant [31]. These two reactions enjoy the unique merits of mild condition, facile operation and good yields. The chemical structure and purity of compounds **1** and **2** were confirmed by ^{1}H and ^{13}C NMR (Fig. S1-S4) and ESI-MS spectra.

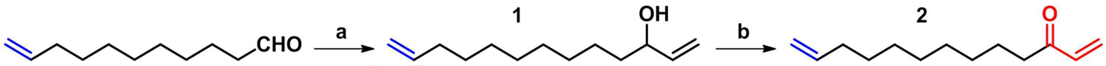

Scheme 1. Monomer synthesis. *Reagents and conditions*: a) 1.5 equiv. vinylmagnesium bromide (1 mol L^{-1} in THF), dry THF, -20 °C to 0 °C, 1 h; b) 1.2 equiv. IBX (0.8 mol L^{-1} in DMSO), THF, rt, 2 h.

3.2. Thiol-Michael model reactions

Vinyl ketone and α-olefin groups are anticipated to undergo cross-metathesis reaction to generate α,β-unsaturated ketones. In order to examine the feasibility of post-polymerization modification of unsaturated polyketone, as shown in Scheme 2, model reactions were conducted by using four types of thiols as nucleophiles. The occurrence of thiol-Michael addition between 3-octen-2-one and 1-butanethiol, benzyl mercaptan, methyl thioglycolate and 4-methylthiophenol indicates the feasibility of post-polymerization modification. Specifically, methyl thioglycolate showed the strongest nucleophilicity since only a slight excess of thiol (120 mol% with respect to 3-octen-2-one) enabled full conversion of the substrate. Meanwhile, 1-butanethiol and benzyl mercaptan both allowed full conversion of 3-octen-2-one although excessive thiols (200 mol% with respect to the substrate) were basically required. Owing to the moderate nucleophilicity of 4-methylthiophenol, only 40% conversion of 3-octen-2-one was observed under the same condition. In spite of this, quantitative conversion of 3-octen-2-one could be realized if a large excess of 4-methylthiophenol (600 mol% with respect to the substrate) was used. In this study, DMF was selected as the solvent to promote Michael addition [32]. Moreover, DMPP instead of amine was selected as the catalyst in order to prevent imine formation [33]. The structures and purity of model compounds were verified by ^{1}H and ^{13}C NMR spectra as shown in Fig. S5-S12. Notably, thioketal was not detected in any case.

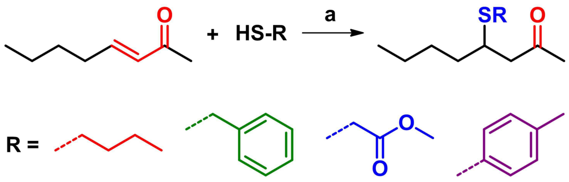

Scheme 2. Model reaction. *Reagents and condition*: a) thiol (see Experimental section for detail), 1 mol% DMPP, DMF, rt, 24 h.

3.3. Optimization of CMP condition

Inspired by CMP systems involving monomers containing α-olefin and acrylate as metathetically polymerizable groups [34-69], as shown in Scheme 3, we envision that generation of unsaturated polyketone **P0** via CMP of AB-type monomer **2** is feasible. Likewise, the occurrence of CMP is motivated by the high cross-metathesis tendency between vinyl ketone and α-olefin groups. In this way, internal vinyl ketone units are periodically incorporated on polymer main chain. As depicted in Table 1, a variety of experimental parameters were examined to optimize the CMP condition with an aim to increase the $M_{n,NMR}$ of **P0**. HG-II catalyst was selected due to its wide application in cross-metathesis reaction [70]. BQ was used in order to suppress olefin isomerization although this inhibitor generally showed negative effect on M_n [71,72]. The solvent for polymerization should be screened so as to meet the requirements of polymer solubility and high catalyst activity. Finally, a suitable polymerization temperature ought to be determined depending on the compromise among reaction rate, solvent evaporation rate and polymer viscosity.

Scheme 3. Synthesis of **P0** via CMP of monomer **2**.

Table 1

Optimization of CMP condition for the synthesis of **P0**.

run	cat [a] [mol%]	BQ [b]	solvent	T [c] [°C]	time [h]	$M_{n,NMR}$ [d]
1	0.5	yes	TOL	80	12	3600
2	0.5	yes	DCM	40	6	2000

3	0.5	yes	DCM	40	12	2400
4	0.5	no	DCM	40	12	3600
5	0.5	yes	TCM	60	12	6200
6	0.5	no	TCM	60	24	7800
7	1.0	no	TCM	60	24	8600

[a] Feed ratio of HG-II with respect to monomer **2**.

[b] 1.0 mol% BQ with respect to monomer **2**.

[c] Polymerization temperature.

[d] Calculated based on terminus analysis. See Fig. S13 for detail.

The conductance of CMP in toluene (which evaporated rather slowly) at 80 ^{o}C (at which polymer was soluble and catalyst decomposition was negligible) resulted in moderate $M_{n,NMR}$ of **P0** (run 1), which was due to the relatively low activity of HG-II in toluene [73]. Indeed, HG-II generally exhibited high activity in DCM. Run 2-4 jointly showed that prolonged reaction time and no addition of BQ were beneficial for the increase of $M_{n,NMR}$. However, rapid evaporation of DCM led to polymer precipitation, so that the formation of high molecular weight polymer was inaccessible. Notably, proton signals of olefin isomerization were not detected even if no BQ was used. A significant increase of $M_{n,NMR}$ was observed if TCM was selected as the solvent (run 5), which might be best explained as the relatively high activity of HG-II and high concentration of CMP system as a solution. Small amount of TCM was intermittently added to prevent polymer precipitation. Encouraged by this, we conducted further optimization. A final $M_{n,NMR}$ of 8600 was achieved by increasing the amount of HG-II and prolonging polymerization time. Hence, run 7 was determined as the standard condition. Once again, the system was confirmed to be free from olefin isomerization. $M_{n,NMR}$ values of run 1-7 were calculated based on terminus analysis of each relevant ^{1}H NMR spectrum (Fig. S13).

3.4. Polymerization kinetics

Chemical structure and molar mass of **P0** (run 7 in Table 1) was monitored by NMR and GPC, respectively. Data of kinetic analysis is collected in Table 2. Samples were taken at certain time interval followed by termination and removal of volatiles prior to characterization. Relative amounts of proton signals denoting α-olefins and vinyl ketones were equally defined as 100%. As shown in Table 2, the polymerization reached almost completion after 24 h, which was slower than the systems employing monomers bearing α-olefin and acrylate terminuses [74-76]. As expected, signals of cross-metathesis (CM) prevail in the CMP process, while those of residual terminuses are marginal. In a mechanistic point of view, kinetically favored self-metathesis (SM) of α-olefins rapidly yields SM dimer. Subsequently, CM between internal alkenes and terminal vinyl ketones gives rise to intermediates bearing internal vinyl ketone units. Notably, relative amount of CM proton signals was 86.2% when the polymerization proceeded for just 0.5 h and finally reached 92.0% when the reaction was terminated at 24 h. This observation indicates that CM overwhelms SM of α-olefins in a rather short time and then proceeds sluggishly to almost completion. Signals of residual terminuses decreased over time, reflecting a gradual increase of molecular weight. It is notable that proton signal of SM indicates the existence of side reaction during polymerization procedure and structural defect within polymer. Incomplete CM between vinyl ketone and 1,2-disubstituted alkene groups along with marginal SM of vinyl ketones (generally considered as SM inactive groups) are responsible for such undesired signals. Unreacted vinyl ketones and SM of α-olefins prevail in terminus structures and structural defects, respectively. These results can be attributed to the priority of SM of α-olefins although SM and CM occur simultaneously throughout the polymerization. Thus, CM indeed dominates in microstructure of **P0** but by no means precludes side reaction such as SM, and alternation index P should never reach 100%. The internal vinyl ketone moieties of **P0** predominantly adopted *trans* configuration. NMR spectra associated with kinetic analysis were collected in Fig. S14, and chemical structure of **P0** was evidenced by ^{1}H and ^{13}C NMR spectra (Fig. S15 and S16).

Table 2

Kinetic analysis of **P0**.

time [h]	α-olefin[a]			vinyl ketone[a]			P^b	$M_{n,NMR}$[c]	$M_{n,GPC}$[d]	$Đ$[d]
	residue	SM	CM	residue	SM	CM				
0.5	6.0%	7.8%	86.2%	11.6%	2.2%	86.2%	94.2%	3300	4700	1.60
1.0	4.0%	7.5%	88.5%	9.4%	2.1%	88.5%	94.3%	4000	5700	1.81
2.0	3.2%	7.5%	89.3%	8.0%	2.7%	89.3%	94.2%	5000	7100	2.03
3.0	2.9%	7.6%	89.5%	7.8%	2.7%	89.5%	94.5%	5200	7400	2.11

4.0	2.6%	7.2%	90.2%	7.8%	2.0%	90.2%	94.2%	5700	8100	2.15
6.0	2.5%	7.3%	90.2%	7.2%	2.6%	90.2%	94.2%	6000	8600	2.25
8.0	2.1%	7.1%	90.8%	6.7%	2.5%	90.8%	94.5%	6400	9100	2.36
12.0	1.9%	7.1%	91.0%	6.6%	2.4%	91.0%	94.5%	7100	10100	2.44
24.0	1.4%	6.7%	91.9%	5.4%	2.7%	91.9%	94.3%	8600	12300	2.49
24.0[e]	1.1%	6.9%	92.0%	5.1%	2.9%	92.0%	94.4%	9800	14000	2.47

[a] Relative molar fraction of olefins calculated based on proton signal integration ratios.

[b] Alternation index, calculated based on integration ratio between signals of CM and SM.

[c] Calculated based on terminus analysis.

[d] Measured by GPC (1 mL min^{-1} in THF at 35 ^{o}C) using polystyrene calibration.

[e] After precipitation.

$M_{n,NMR}$ is calculated based on integration ratio among proton signals of residual terminus, SM and CM. A final $M_{n,NMR}$ value of 9800 is reached after precipitation. Meanwhile, GPC results show that $M_{n,GPC}$ value increased over time (Fig. S17 and S18), and the trend coincide well with that of $M_{n,NMR}$. Finally, high value of polydispersity (*Đ*) is in consistent with step-growth mechanism.

3.5. Post-polymerization modification

As shown in Scheme 4, post-polymerization modification of **P0** was conducted via thiol-Michael chemistry [77] to afford functional polymers **P1**-**P6**. Full conversion of the internal vinyl ketone groups of **P0** was achieved by using thiols **T1**-**T6** although excessive thiol, elevated temperature and prolonged reaction time were basically required in each case. First of all, polymers **P1**-**P4** were synthesized to examine the efficacy of post-polymerization modification by employing thiols **T1**-**T4**, which were previously investigated in model reaction study. Chemical structures of **P1**-**P4** were confirmed by ^{1}H (Fig. 1) and ^{13}C (Fig. S19) NMR spectra. Complete disappearance of the proton signals of terminal and internal vinyl ketone groups verifies full conversion of these Michael acceptors. Internal, terminal and SM vinyl ketone moieties were apparently identical in chemical reactivity whereas terminal and SM α-olefin groups were inert to post-polymerization modification. Moreover, proton signal of thioketal unit cannot be detected. The integration ratios among all the characteristic proton signals are highly consistent with predicted values. The ^{1}H, ^{13}C and ^{19}F NMR spectra of polymers **P5** and **P6** are shown in Fig. S20-S22.

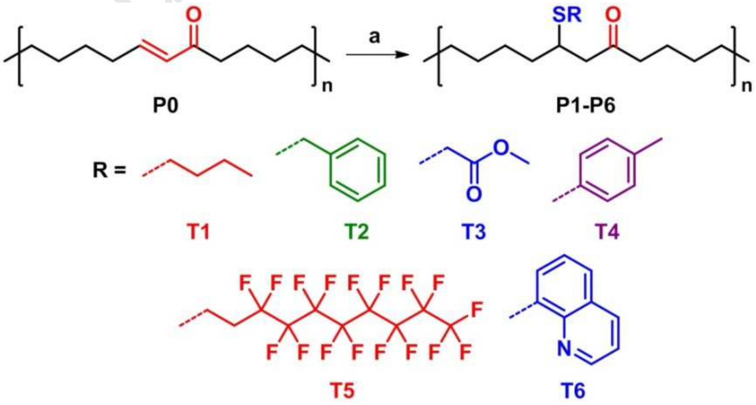

Scheme 4. Synthesis of **P1**-**P6** via post-polymerization modification of **P0**. *Reagents and condition*: a) 6 equiv. thiol, 1 mol% DMPP, TCM/DMF, 50 °C, 48 h.

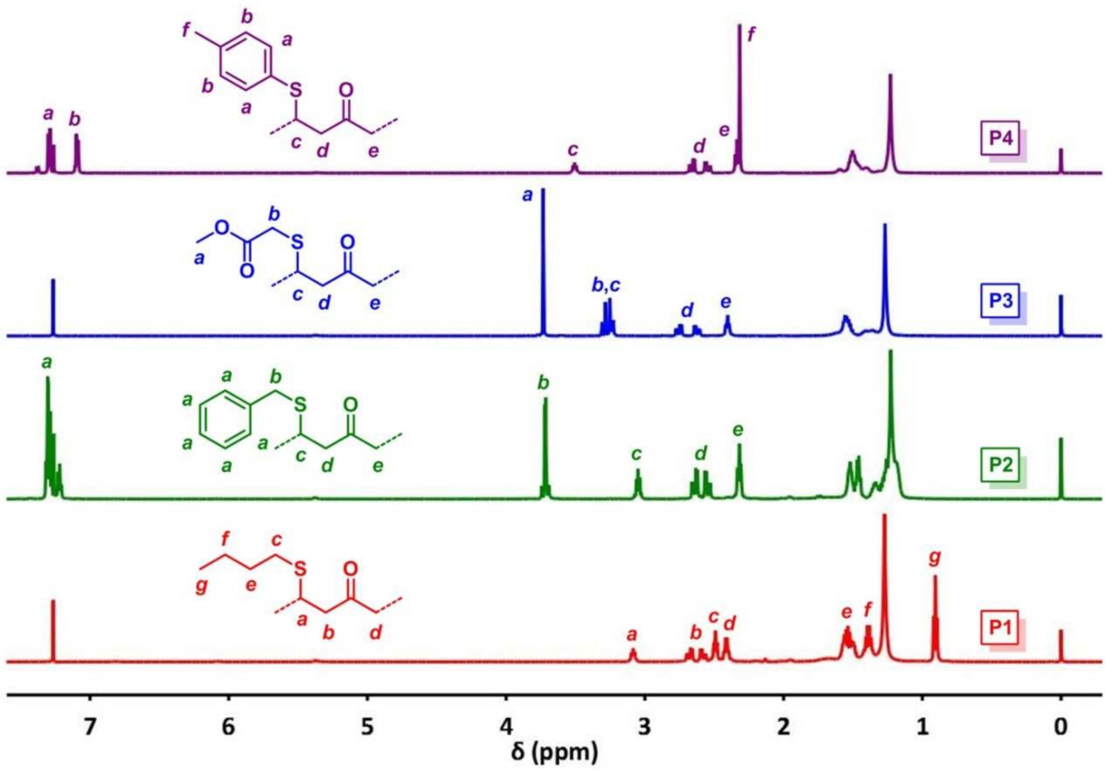

Fig. 1. ^{1}H NMR spectra of **P1**-**P4** in $CDCl_3$ (structures of side chains shown and characteristic peaks designated only).

We moved on to investigate the molecular weights and thermal properties of polymers **P0**-**P4**. As shown in Table 3, polymers **P0**-**P4** show similar $M_{n,GPC}$, indicating that hydrodynamic radiuses of these polymers are very close. Moreover, this system is free from chain scission or cross-linking. The relatively low $Đ$ values of polymers **P1**-**P4** are due to repetitive precipitation, during which the fractions of low molecular weight components are reduced.

Table 3

Molecular weight and thermal data of **P0**-**P4**.

entry	$M_{n,GPC}$[a]	$Đ$[a]	T_g [b] [^oC]	T_m [b] [^oC]	T_d [c] [^oC]
P0	12300	2.49	-1.5	86.3	394
P1	12200	1.96	-57.7	n.d.[d]	-[e]
P2	13000	1.91	-57.1	n.d.	-
P3	14500	1.94	-57.2	n.d.	-
P4	13800	1.93	-57.6	n.d.	-

[a] Determined by GPC (1 ml min^{-1} in THF at 35 ^oC) using polystyrene calibration.

[b] Determined by DSC, 10 °C min^{-1} scan rate. Values were recorded from second scan data.

[c] Determined by TGA, 10 °C min^{-1} scan rate. T_d is defined as the temperature at 5% weight loss.

[d] Not detected.

[e] Not measured.

As for thermal properties, polymer **P0** shows relatively high T_g due to the rigidity of vinyl ketone groups. On the contrary, the T_gs of polymers **P1**-**P4** significantly decrease after thiol-Michael addition, which is due to the flexibility of polymer chain induced by saturation. To our interest, polymers **P1**-**P4** exhibit nearly identical T_gs, suggesting that the T_g of the functional polyketone is irrelevant to the type of side group for this system. Meanwhile, the crystallinity of **P0** is evidenced by DSC and WAXD results (Fig. S23 and S24), and this polymer shows a unique melting peak at 86.3 ^oC. On the contrary, the absence of melting peak for polymers **P1**-**P4** might be best explained as the irregular packing of polymer chain caused by bulky side groups. In addition, polymer **P0** exhibits high thermal stability, whereas the T_ds of polymers

P1-**P4** are not measured in this contribution so as to prevent the release of odorous sulfur-containing substances. The TGA curve of **P0** is shown in Fig. S25.

In order to expand the potential application areas of this synthetic methodology, post-polymerization modification of polymer **P0** was conducted by using thiols **T5** and **T6** to yield hydrophobic (**P5**) and fluorescent (**P6**) polyketones, respectively. First of all, water contact angles of **P0** and **P5** were measured to examine the wettability of surfaces that coated with these polymers. Fig. 2A shows that the hydrophobicity of polymer **P5** is more pronounced due to the existence of perfluorocarbon pendent groups. The data of different measurements shows consistent result. It is anticipated that the wettability of polyketone can be altered by using different thiols. Moreover, superhydrophobic surface can also be fabricated if the roughness is increased [78].

UV-Vis absorption and fluorescence emission spectra of polymer **P6** are recorded to establish correlation between concentration and spectroscopic property. As shown in Fig. 2B and 2C, the UV-Vis absorbance at 340 nm displays linear relationship with concentration of **P6** in the range from 77.2 μmol L^{-1} to 3.67 mmol L^{-1}. On the other hand, polymer **P6** shows concentration-dependent fluorescence intensity as revealed by Fig. 2D-2F. Specifically, the fluorescence intensity enhances while increasing the concentration of polymer **P6** from 77.2 μmol L^{-1} to 1.84 mmol L^{-1} but decreases if the concentration is higher than 1.84 mmol L^{-1}. As expected, the increase of fluorophore concentration should increase the fluorescence intensity. Nevertheless, fluorescence quenching may occur if the concentration exceeds some critical value [79,80]. In this study, the critical value appears to be 1.84 mmol L^{-1}. Noteworthy, the fluorescence intensity of polymer **P6** shows plausible linear relationship with concentration in the range from 77.2 μmol L^{-1} to 617.6 μmol L^{-1}. Moreover, blue emission was observed under UV light (365 nm irradiation by handheld UV lamp, concentration of **P6** being 1.84 mmol L^{-1}), indicating that polymer **P6** is a practical fluorescent probe.

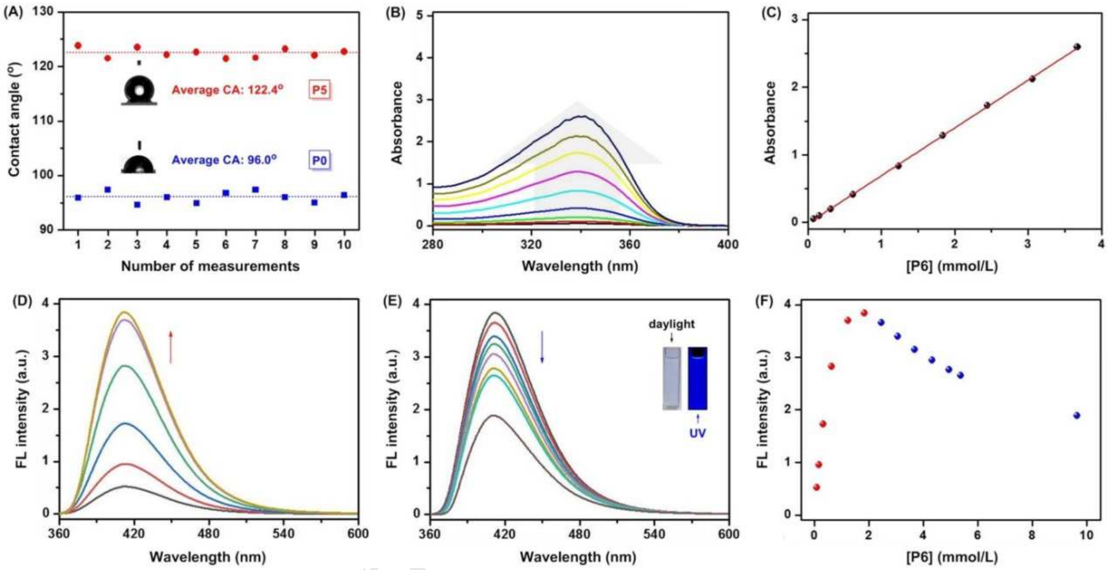

Fig. 2. (A) Contact angle images and data for droplets of water on **P0** and **P5** surfaces. (B) UV-Vis spectra of **P6** in TCM at room temperature. (C) Linear plots of absorbance versus different concentrations of **P6** at 340 nm. [**P6**] is calculated based on its monomer unit. (D) and (E) Fluorescence spectra of **P6** in TCM at room temperature. Optical images are inserted (under daylight and irradiation by UV lamp, E_x = 365 nm, respectively). (F) Plots of fluorescence intensity versus different concentrations of **P6** at 412 nm.

4. Conclusions

In this study, we report the synthesis of aliphatic polyketones via sequential CMP and thiol-Michael chemistry. First of all, bio-based monomer **2** was synthesized in two steps by using natural product derivative 10-undecenal as the starting material. The results of model reaction verified the feasibility of Michael addition between 3-octen-2-one and thiol compounds. Optimization of CMP condition was carried out to afford high molecular weight **P0** ($M_{n,GPC}$ = 14 kDa). Moreover, the results of kinetic study demonstrated high efficiency and structural fidelity of this system. Finally, post-polymerization modification of pristine polyketone **P0** by using thiol-Michael addition readily yielded functional polyketones **P1**-**P6**. Full conversion of the internal vinyl ketone groups of **P0** was observed in each case. In particular, the fabrication of hydrophobic and fluorescent polyketones **P5** and **P6** indicated the huge potential of this synthetic protocol for the synthesis of a diverse range of functional polyketones.

Acknowledgements

F.-R.Z. and J.X. contributed equally to this work. The authors appreciate financial support from the Open Project Program of Beijing National Laboratory for Molecular Sciences (BNLMS201808) and the National Natural Science Foundation of China (No. 21504027).

Appendix A. Supplementary data

Supplementary data related to this article can be found at http://dx.doi.org/10.1016/j.polymer.201X.XX.XXX.

References

[1] L.S. Boffa, B.M. Novak, Copolymerization of polar monomers with olefins using transition-metal complexes, Chem. Rev. (100) 2000 1479-1494.

[2] A. Nakamura, S. Ito, K. Nozaki, Coordination-insertion copolymerization of fundamental polar monomers, Chem. Rev. (109) 2009 5215-5244.

[3] L. Guo, W. Liu, C. Chen, Late transition metal catalyzed α-olefin polymerization and copolymerization with polar monomers, Mater. Chem. Front. (1) 2017 2487-2494.

[4] A. Nakamura, T.M.J. Anselment, J. Claverie, B. Goodall, R.F. Jordan, S. Mecking, B. Rieger, A. Sen, P.W.N.M. van Leeuwen, K. Nozaki, *Ortho*-Phosphinobenzenesulfonate: A superb ligand for palladium-catalyzed coordination-insertion copolymerization of polar vinyl monomers, Acc. Chem. Res. (46) 2013 1438-1449.

[5] G.H. Hartley, J.E. Guillet, Photochemistry of ketone polymers. I. Studies of ethylene-carbon monoxide copolymers, Macromolecules (1) 1968 165-170.

[6] M.M. Brubaker, D.D. Coffman, H.H. Hoehn, Synthesis and characterization of ethylene/carbon monoxide copolymers, a new class of polyketones, J. Am. Chem. Soc. 74 (1952) 1509-1515.

[7] E. Drent, J.A.M. van Broekhoven, M.J. Doyle, Efficient palladium catalysts for the copolymerization of carbon monoxide with olefins to produce perfectly alternating polyketones, J. Organomet. Chem. 417 (1991) 235-251.

[8] E. Drent, R. van Dijk, R. van Ginkel, B. van Oort, R.I. Pugh, The first example of palladium catalysed non-perfectly alternating copolymerisation of ethene and carbon monoxide, Chem. Commun. (2002) 964-965.

[9] A.K. Hearley, R.J. Nowack, B. Rieger, New single-site palladium catalysts for the nonalternating copolymerization of ethylene and carbon monoxide, Organometallics 24 (2005) 2755-2763.

[10] L. Bettucci, C. Bianchini, C. Claver, E.J. Garcia Suarez, A. Ruiz, A. Meli, W. Oberhauser, Ligand effects in the non-alternating CO-ethylene copolymerization by palladium(II) catalysis, Dalton Trans. (2007) 5590-5602.

[11] D.K. Newsham, S. Borkar, A. Sen, D.M. Conner, B.L. Goodall, Inhibitory role of carbon monoxide in palladium(II)-catalyzed nonalternating ethene/carbon monoxide copolymerizations and the synthesis of polyethene-*block*-poly(ethene-*alt*-carbon monoxide), Organometallics 26 (2007) 3636-3638.

[12] R. Luo, D.K. Newsham, A. Sen, Palladium-catalyzed nonalternating copolymerization of ethene and carbon monoxide: Scope and mechanism, Organometallics 28 (2009) 6994-7000.

[13] E.J. García Suárez, C. Godard, A. Ruiz, C. Claver, Alternating and non-alternating Pd-catalysed co- and terpolymerisation of carbon monoxide and alkenes, Eur. J. Inorg. Chem. (2007) 2582-2593.

[14] J. Huang, F.-B. Li, J. Zou, G.-Q. Yuan, X.-L. Shi, D.-S. Yu, Polyketone from ethylene with carbon monoxide catalyzed by novel catalyst systems based on copper with bidentate phosphorus chelating ligands, Chin. J. Polym. Sci. 21 (2003) 479-481.

[15] E. Drent, P.H.M. Budzelaar, Palladium-catalyzed alternating copolymerization of alkenes and carbon monoxide, Chem. Rev. 96 (1996) 663-682.

[16] S. DeVito, S. Bronco, A thermogravimetric study of the effect of palladium catalyst residue on the degradation of ethylene-carbon monoxide alternating copolymer, Polym. Degrad. Stab. 63 (1999) 399-406.

[17] D. Takeuchi, K. Watanabe, K. Osakada, Synthesis of polyketones containing substituted six-membered rings via Pd-catalyzed copolymerization of methylenecyclohexanes with

carbon monoxide, Macromolecules 48 (2015) 6745-6749.

[18] S.S. Soomro, D. Cozzula, W. Leitner, H. Vogt, T.E. Müller, The microstructure and melt properties of CO-ethylene copolymers with remarkably low CO content, Polym. Chem. 5 (2014) 3831-3837.

[19] C.W. Bielawski, R.H. Grubbs, Living ring-opening metathesis polymerization, Prog. Polym. Sci. 32 (2007) 1-29.

[20] L. Caire da Silva, G. Rojas, M.D. Schulz, K.B. Wagener, Acyclic diene metathesis polymerization: History, methods and applications, Prog. Polym. Sci. 69 (2017) 79-107.

[21] M.D. Watson, K.B. Wagener, Tandem homogeneous metathesis/heterogeneous hydrogenation: Preparing model ethylene/CO_2 and ethylene/CO copolymers, Macromolecules 33 (2000) 3196-3201.

[22] P. Ortmann, F.P. Wimmer, S. Mecking, Long-spaced polyketones from ADMET copolymerizations as ideal models for ethylene/CO copolymers, ACS Macro Lett. 4 (2015) 704-707.

[23] K.J. Arrington, C.B. Murray, E.C. Smith, H. Marand, J.B. Matson, Precision polyketones by ring-opening metathesis polymerization: Effects of regular and irregular ketone spacing, Macromolecules 49 (2016) 3655-3662.

[24] K.J. Arrington, J.B. Waugh, S.C. Radzinski, J.B. Matson, Photo- and biodegradable thermoplastic elastomers: Combining ketone-containing polybutadiene with polylactide using ring-opening polymerization and ring-opening metathesis polymerization, Macromolecules 50 (2017) 4180-4187.

[25] F.-R. Zeng, Q.-L. Zhu, Z.-L. Li, Sequential modification of ADMET polyketone via oxime

chemistry and electrophilic alkoxyetherification, Aust. J. Chem. 71 (2018) 449-454.

[26] M. Van der Steen, C.V. Stevens, Y. Eeckhout, L. De Buyck, F. Ghelfi, F. Roncaglia, Undecylenic acid: A valuable renewable building block on route to Tyromycin A derivatives, Eur. J. Lipid Sci. Technol. 110 (2008) 846-852.

[27] G. Das, R.K. Trivedi, A.K. Vasishtha, Heptaldehyde and undecylenic acid from castor oil, J. Am. Oil Chem. Soc. 66 (1989) 938-941.

[28] O. Kreye, T. Tóth, M.A.R. Meier, Poly-α,β-unsaturated aldehydesderived from castor oil *via* ADMET polymerization, Eur. J. Lipid Sci. Technol. 113 (2011) 31-38.

[29] X. Miao, C. Fischmeister, C. Bruneau, P.H. Dixneuf, A direct route to bifunctional aldehyde derivatives via self- and cross-metathesis of unsaturated aldehydes, ChemSusChem 2 (2009) 542-545.

[30] A.K. Chatterjee, T.-L. Choi, D.P. Sanders, R.H. Grubbs, A general model for selectivity in olefin cross metathesis, J. Am. Chem. Soc. 125 (2003) 11360-11370.

[31] G.A. Molander, L. Jean-Gérard, Scope of the Suzuki-Miyaura cross-coupling reaction of potassium trifluoroboratoketohomoenolates, J. Org. Chem. 74 (2009) 1297-1303.

[32] D.P. Nair, M. Podgórski, S. Chatani, T. Gong, W. Xi, C.R. Fenoli, C.N. Bowman, The thiol-Michael addition click reaction: A powerful and widely used tool in materials chemistry, Chem. Mater. 26 (2014) 724-744.

[33] M.E. Belowich, J. Fraser Stoddart, Dynamic imine chemistry, Chem. Soc. Rev. 41 (2012) 2003-2024.

[34] Y. Liang, F.-R. Zeng, Z.-L. Li, Precision aliphatic polyesters *via* cross-metathesis polymerization, Curr. Org. Syn. 16 (2019) 188-204.

[35] F. Sinclair, L. Chen, B.W. Greenland, M.P. Shaver, Installing multiple functional groups on biodegradable polyesters via post-polymerization olefin cross-metathesis, Macromolecules 49 (2016) 6826-6834.

[36] F. Sinclair, M. Alkattan, J. Prunet, M.P. Shaver, Olefin cross metathesis and ring-closing metathesis in polymer chemistry, Polym. Chem. 8 (2017) 3385-3398.

[37] S.D. Morrison, R.M.J. Liskamp, J. Prunet, Tailoring polyethers for post-polymerization functionalization by cross metathesis, Org. Lett. 20 (2018) 2253-2256.

[38] M.D. Schulz, R.R. Ford, K.B. Wagener, Insertion metathesis depolymerization, Polym. Chem. 4 (2013) 3656-3658.

[39] Y. Dong, J.B. Matson, K.J. Edgar, Olefin cross-metathesis in polymer and polysaccharide chemistry: A review, Biomacromolecules 18 (2017) 1661-1676.

[40] T.-L. Choi, I.M. Rutenberg, R.H. Grubbs, Synthesis of A,B-alternating copolymers by ring-opening-insertion-metathesis polymerization, Angew. Chem. Int. Ed. 41 (2002) 3839-3841.

[41] S. Demel, C. Slugovc, F. Stelzer, K. Fodor-Csorba, G. Galli, Alternating diene metathesis polycondensation (ALTMET) - a versatile tool for the preparation of perfectly alternating AB copolymers. Macromol. Rapid Commun. 24 (2003) 636-641.

[42] L. Ding, M. Xu, J. Wang, Y. Liao, J. Qiu, Controlled synthesis of azobenzene functionalized homo and copolymers via direct acyclic diene metathesis polymerization, Polymer 55 (2014) 1681-1687.

[43] L. Ding, X.-Q. Zheng, R. Lu, J. An, J. Qiu, Perfectly AB-alternating copolymers via alternating diene metathesis polymerization: one-step synthesis, characterization and properties, Polym.

Int. 63 (2014) 997-1002.

[44] H.-K. Lee, K.-T. Bang, A. Hess, R.H. Grubbs, T.-L. Choi, Multiple olefin metathesis polymerization that combines all three olefin metathesis transformations: Ring-opening, ring-closing, and cross metathesis, J. Am. Chem. Soc. 137 (2015) 9262-9265.

[45] M. Winkler, L.M. de Espinosa, C. Barner-Kowollik, M.A.R. Meier, A new approach for modular polymer-polymer conjugations *via* Heck coupling, Chem. Sci. 3 (2012) 2607-2615.

[46] M. Winkler, J.O. Mueller, K.K. Oehlenschlaeger, L.M. de Espinosa, M.A.R. Meier, C. Barner-Kowollik, Highly orthogonal functionalization of ADMET polymers via photo-induced Diels-Alder reactions, Macromolecules 45 (2012) 5012-5019.

[47] L. Ding, C. Wang, L. Lin, Z. Zhu, One-pot sequential ring-opening metathesis polymerization and acyclic diene metathesis polymerization synthesis of unsaturated block polyphosphoesters, Macromol. Chem. Phys. 216 (2015) 761-769.

[48] A. Sehlinger, L.M. de Espinosa, M.A.R. Meier, Synthesis of diverse asymmetric α,ω-dienes via the Passerini three-component reaction for head-to-tail ADMET polymerization, Macromol. Chem. Phys. 214 (2013) 2821-2828.

[49] L. Ding, R. Lu, J. An, X. Zheng, J. Qiu, Cyclic polyphosphoesters synthesized by acyclic diene metathesis polymerization and ring closing metathesis, React. Funct. Polym. 73 (2013) 1242-1248.

[50] L. Ding, W. Song, R. Jiang, L. Zhu, Macrocycle-based topological azo-polymers: Facile synthesis and unusual photoresponsive properties, Polym. Chem. 8 (2017) 7133-7142.

[51] L.M. de Espinosa, M.A.R. Meier, Synthesis of star- and block-copolymers using ADMET: Head-to-tail selectivity during step-growth polymerization, Chem. Commun. 47 (2011)

1908-1910.

[52] L.M. de Espinosa, M. Winkler, M.A.R. Meier, Acyclic diene metathesis polymerization and Heck polymer-polymer conjugation for the synthesis of star-shaped block copolymers, Macromol. Rapid Commun. 34 (2013) 1381-1386.

[53] M. Unverferth, M.A.R. Meier, Tuning the polarity of ADMET derived star-shaped polymers *via* thiol-ene chemistry, Polymer 55 (2014) 5571-5575.

[54] J. Qiu, J. Zhang, F. Yu, J. Wei, L. Ding, Novel ABC miktoarm star terpolyphosphoesters: Facile construction and high-flame retardant property, J. Polym. Sci., Part A: Polym. Chem. 54 (2016) 692-701.

[55] L. Ding, J. Wei, J. Qiu, J. Wang, Z. Zhu, Star-shaped polyphosphoesters with reactive end groups synthesized *via* acyclic diene metathesis polymerization and their transformation to nanostructures, RSC Adv. 4 (2014) 22342-22349.

[56] L. Ding, C. Wang, R. Jiang, L. Wang, W. Song, Preparation of small and photoresponsive polymer nanoparticles by intramolecular crosslinking of reactive star azo-polymers, React. Funct. Polym. 109 (2016) 56-63.

[57] L. Ding, J. Li, T. Li, L. Zhang, W. Song, Linear, Y-shaped, and H-shaped amphiphilic azobenzene copolymers: Facile synthesis and topological effect on self-assembly and photoresponsive property, React. Funct. Polym. 121 (2017) 15-22.

[58] L. Ding, J. Qiu, J. Li, C. Wang, L. Wang, Novel photoresponsive linear, graft, and comb-like copolymers with azobenzene chromophores in the main-chain and/or side-chain: Facile one-pot synthesis and photoresponse properties, Macromol. Rapid Commun. 36 (2015) 1578-1584.

[59] L. Ding, J. Qiu, J. Wei, Z. Zhu, Convenient divergent synthesis of linear-dendron block polyphosphoesters *via* acyclic diene metathesis polymerization, Polym. Chem. 5 (2014) 4285-4292.

[60] I.A. Gorodetskaya, T.-L. Choi, R.H. Grubbs, Hyperbranched macromolecules via olefin metathesis, J. Am. Chem. Soc. 129 (2007) 12672-12673.

[61] I.A. Gorodetskaya, A.A. Gorodetsky, E.V. Vinogradova, R.H. Grubbs, Functionalized hyperbranched polymers via olefin metathesis, Macromolecules 42 (2009) 2895-2898.

[62] L. Ding, L. Zhang, H. Han, W. Huang, C. Song, M. Xie, Y. Zhang, Hyperbranched azo-polymers synthesized by acyclic diene metathesis polymerization of an AB_2 monomer, Macromolecules 42 (2009) 5036-5042.

[63] L. Ding, M. Xie, D. Yang, C. Song, Efficient synthesis of long-chain highly branched polymers via one-pot tandem ring-opening metathesis polymerization and acyclic diene metathesis polymerization, Macromolecules 43 (2010) 10336-10342.

[64] L. Ding, G. Yang, M. Xie, D. Gao, J. Yu, Y. Zhang, More insight into tandem ROMP and ADMET polymerization for yielding reactive long-chain highly branched polymers and their transformation to functional polymer nanoparticles, Polymer 53 (2012) 333-341.

[65] M. Xie, L. Ding, Z. You, D. Gao, G. Yang, H. Han, Robust hybrid nanostructures comprising gold and thiol-functionalized polymer nanoparticles: Facile preparation, diverse morphologies and unique properties, J. Mater. Chem. 22 (2012) 14108-14118.

[66] N. Wang, L. Ding, Cyclodextrin-based hyperbranched polymers by acyclic diene metathesis polymerization of an AB_n monomer: Molecule design, synthesis, and characterization, J. Polym. Res. 19 (2012) 9863.

[67] L. Ding, J. Qiu, R. Lu, X. Zheng, J. An, Hyperbranched polyphosphoesters with reactive end groups synthesized via acyclic diene metathesis polymerization and their transformation to crosslinked nanoparticles, J. Polym. Sci., Part A: Polym. Chem. 51 (2013) 4331-4340.

[68] L. Ding, L. Lin, C. Wang, J. Qiu, Z. Zhu, Facile synthesis of linear-hyperbranched polyphosphoesters via one-pot tandem ROMP and ADMET polymerization and their transformation to architecturally defined nanoparticles, J. Polym. Sci., Part A: Polym. Chem. 53 (2015) 964-972.

[69] O. Kreye, D. Kugele, L. Faust, M.A.R. Meier, Divergent dendrimer synthesis via the Passerini three-component reaction and olefin cross-metathesis, Macromol. Rapid Commun. 35 (2014) 317-322.

[70] S.B. Garber, J.S. Kingsbury, B.L. Gray, A.H. Hoveyda, Efficient and recyclable monomeric and dendritic Ru-based metathesis catalysts, J. Am. Chem. Soc. 122 (2000) 8168-8179.

[71] S.H. Hong, D.P. Sanders, C.W. Lee, R.H. Grubbs, Prevention of undesirable isomerization during olefin metathesis, J. Am. Chem. Soc. 127 (2005) 17160-17161.

[72] P.A. Fokou, M.A.R. Meier, Studying and suppressing olefin isomerization side reactions during ADMET polymerizations, Macromol. Rapid Commun. 31 (2010) 368-373.

[73] M.D. Schulz, K.B. Wagener, Solvent effects in alternating ADMET polymerization, ACS Macro Lett. 1 (2012) 449-451.

[74] Z.-L. Li, F.-R. Zeng, J.-M. Ma, L.-H. Sun, Z. Zeng, H. Jiang, Precision aliphatic polyesters with alternating microstructures via cross-metathesis polymerization: An event of sequence control, Macromol. Rapid Commun. 38 (2017) 1700050.

[75] F.-R. Zeng, J.-M. Ma, L.-H. Sun, Z. Zeng, H. Jiang, Z.-L. Li, Optically active precision aliphatic

polyesters via cross-metathesis polymerization, Macromol. Chem. Phys. 219 (2018) 1800031.

[76] F.-R. Zeng, J.-M. Ma, L.-H. Sun, Z. Zeng, H. Jiang, Z.-L. Li, Hyperbranched aliphatic polyester via cross-metathesis polymerization: Synthesis and postpolymerization modification, Macromol. Rapid Commun. 39 (2018) 1700658.

[77] J.W. Chan, C.E. Hoyle, A.B. Lowe, M. Bowman, Nucleophile-initiated thiol-Michael reactions: Effect of organocatalyst, thiol, and ene, Macromolecules 43 (2010) 6381-6388.

[78] S. Wang, K. Liu, X. Yao, L. Jiang, Bioinspired surfaces with superwettability: New insight on theory, design, and applications, Chem. Rev. 115 (2015) 8230-8293.

[79] C.A. Breen, T. Deng, T. Breiner, E.L. Thomas, T.M. Swager, Polarized photoluminescence from poly(*p*-phenylene-ethynylene) via a block copolymer nanotemplate, J. Am. Chem. Soc. 125 (2003) 9942-9943.

[80] X.P. Zhang, B.Q. Sun, Organic crystal fibers aligned into oriented bundles with polarized emission, J. Phys. Chem. B 111 (2007) 10881-10885.

Highlights

- Cross-metathesis polymerization proves to be an efficient and straightforward method for the synthesis of unsaturated polyketone.
- Post-polymerization modification of pristine polyketone enables the generation of a diverse range of functional polymeric materials.
- Full conversion of the internal alkene units of unsaturated polyketone is realized by using thiol-Michael chemistry.
- A natural product derivative, 10-undecenal, is selected as the starting material for concise synthesis of bio-based monomer.
- Characterization of polyketones can be routinely conducted due to their solubility in most common organic solvents.

Declaration of interests

☒ The authors declare that they have no known competing financial interests or personal relationships that could have appeared to influence the work reported in this paper.

☐The authors declare the following financial interests/personal relationships which may be considered as potential competing interests: